J Mol Model (2014) 20:2413
DOI 10.1007/s00894-014-2413-3

ORIGINAL PAPER

Structural and dynamical properties of Li^+-dibenzo-18-crown-6(DB18C6) complex in pure solvents and at the aqueous-organic interface

Pooja Sahu · Sk. M. Ali · Jayant K. Singh

Received: 29 January 2014 / Accepted: 4 August 2014 / Published online: 17 August 2014

Abstract Microstructure of dibenzo-18-crown-6 (DB18C6) and DB18C6/Li^+ complex in different solvents (water, methanol, chloroform, and nitrobenzene) have been analyzed using radial distribution function (RDF), coordination number (CN), and orientation profiles, in order to identify the role of solvents on complexation of DB18C6 with Li^+, using molecular dynamics (MD) simulations. In contrast to aqueous solution of LiCl, no clear solvation pattern is found around Li^+ in the presence of DB18C6. The effect of DB18C6 has been visualized in terms of reduction in peak height and shift in peak positions of $g_{Li\text{-}Ow.}$ The appearance of damped oscillations in velocity autocorrelation function (VACF) of complexed Li^+ described the high frequency motion to a "rattling" of the ion in the cage of DB18C6. The solvent-complex interaction is found to be higher for water and methanol due to hydrogen bond (HB) interactions with DB18C6. However, the stability of DB18C6/Li^+ complex is found to be almost similar for each solvent due to weak complex-solvent interactions. Further, Li^+ complex of DB18C6 at the liquid/liquid interface of two immiscible solvents confirm the high interfacial activity of DB18C6 and DB18C6/Li^+ complex. The complexed Li^+ shows higher affinity for water than organic solvents; still they remain at the interface rather than migrating toward water due to higher surface tension of water as compared to organic solvents. These simulation results shed light on the role of counter-ions and spatial orientation of species in pure and hybrid solvents in the complexation of DB18C6 with Li^+.

Keywords Dibenzo 18-crown-6 · Interface · Li^+ ion extraction · Molecular dynamics · Solvation effect

Electronic supplementary material The online version of this article (doi:10.1007/s00894-014-2413-3) contains supplementary material, which is available to authorized users.

P. Sahu · J. K. Singh (✉)
Department of Chemical Engineering, Indian Institute of Technology Kanpur, Kanpur, India 208016
e-mail: jayantks@iitk.ac.in

P. Sahu · S. M. Ali (✉)
Chemical Engineering Division, Bhabha Atomic Research Center, Mumbai, India 400085
e-mail: musharaf@barc.gov.in

Introduction

Separation of metal ions is increasingly attracting attention in recent years due to their immense demand in different fields of scientific and technical applications. In the late twentieth century, lithium became an essential part of our life. It is widely used for high temperature performance of electronic devices [1] because of its unique band structure. Lithium in anti-depression medicines [2] is a life saver. The hygroscopic nature of LiCl and LiBr is used to desiccant the gas stream [3], whereas the lithium in form of LiOH and Li_2O_2 is mostly used in spacecraft and submarines for CO_2 absorption [4]. Appropriate composition of lithium and aluminum is used to form light and strong alloys [5] for aerospace applications. Besides all these applications, separation of lithium ions and their isotopes becomes essential because of their key role in nuclear industries especially for fusion reactions in tritium breeder reactor [6]. These increasing end uses of lithium demand an effective separation methodology for lithium ions.

Numerous separation techniques such as use of peat [7], membrane-filtration, bio-filtration [8], adsorption [9], and physico-chemical treatment process [10] have been tested for extraction of metal ions. Benefits and limitations of these processes have been analyzed and are widely reported [11].

Recently, use of crown ethers [12] has become very efficient for separation of metal ions. This is primarily due to the micelle type structure of crown ether, which helps them to

form an inclusive complex with several metal ions. Crown ethers have the ability to bind not only charged guests like metal ions but also to the neutral guest such as water, methanol etc., through the non-covalent interactions of van der Waals force and hydrogen bonding [13, 14]. Crown ethers have also shown potential to separate isotopes [6]. Because of these complexing properties, crown ethers find a wide variety of applications in environmental research especially as the separating agents for removing metal ions and their isotopes from mixed nuclear and chemical wastes. The binding specificities of crown ethers with metal ions have been mainly described in terms of similarities between cation size and the cavity of the crown ethers. However selectivity of crown ether to ions cannot be explained simply by cavity size relationship, but it requires the interplay of interactions among crown ethers, solvents, and the guest molecules [15]. For example, in gas phase, 18-crown-6 (18C6) and dibenzo18-crown-6 (DB18C6) form preferential complexation in the order $Li^+ > Na^+ > K^+ > Rb^+ > Cs^+$; while in aqueous solution both of them show highest complexion capacity for K^+ rather than Li^+ [15].

Numerous experiments have been performed on crown ethers using calorimetric [16], conductometric, capillary electrophoresis [17], and nuclear magnetic resonance techniques [18] to demonstrate the relative stabilities of the complexes formed by crown ethers with ions in different solvents. The results reveal that crown ethers form stable 1:1 complex in most of the solvents. However, its stability depends on the nature and size of the guest and solvent molecules. DB18C6, which is the first crown ether discovered by Pedersen in 1967, is known to display strong and selective binding for alkaline earth metals and alkali metals [19, 20]. Various studies have been devoted to measure the stability constant for complexation of DB18C6 with divalent and univalent cations using density functional theory (DFT) calculations [21]. For example, Heo and co-workers have investigated the selectivity of DB18C6 for charged and neutral guests in aqueous solution using DFT combined with dielectric continuum solvation model [22]. The choice of ligand DB18C6, for separation of Li^+ is mainly supported by quantum calculations and gas phase experimental studies; which have shown the intrinsic binding affinity of DB18C6 for smaller metal ions such as Li^+ and Na^+ [22]. In our earlier studies [23], it has been shown that substituted crown ether works well as compared to unsubstituted crown ether due to reduction in solubility and cavity size but this study was done in single phase and no dynamics for complexed Li^+ was reported. Hence, the study needs to further extended with substituted crown ether DB18C6 for separation of Li^+. Which would be helpful to answer many questions such as—how many solvent molecules does DB18C6 replace from the coordination shell of Li^+? What is the difference between the hydration of Li^+ in bulk and in the complex? What happens at liquid-liquid interface during ion separation? Does the nature of organic solvent in which DB18C6 is dissolved affect the separation process in liquid-liquid extraction? These questions remain unaddressed, which may play a vital role in the selectivity of DB18C6 toward Li^+ in the solutions. In the present study, an effort has been made to elucidate the intrinsic properties of DB18C6, in complex with Li^+ in the solvents such as water, methanol, chloroform, and nitrobenzene. The purpose of this paper is to present a theoretical investigation on the structural and energetic aspects of Li^+ selectivity, in terms of intrinsic binding features of the DB18C6 and solvation effects. We have also studied the interfacial behavior of liquid-liquid interface in the presence of DB18C6 in order to understand the transfer mechanism of metal ions across liquid interface. The effect of counter ions and the nature of organic solvents on the interfacial activity of DB18C6 have also been studied to investigate the interfacial behavior of DB18C6, in relation with its ionophoric properties with Li^+.

Model and methodology

Model

All atom OPLS force field model is adopted to represent solvents: methanol [24], chloroform [25], and nitrobenzene [26]. However, for water we have used TIP4P/2005 model [27] as it was found to provide good agreement with the experimental EXAFS spectrum in compared to the other water models [28]. In the case of water, bond distance and bond angle are fixed throughout the simulation with SHAKE algorithm [29]. The intermolecular interaction between the atoms is defined as:

$$U(r_{ij}) = 4\varepsilon_{ij}\left[\left(\frac{\sigma_{ij}}{r_{ij}}\right)^{12} - \left(\frac{\sigma_{ij}}{r_{ij}}\right)^{6}\right] + \sum_{i=1}^{3}\sum_{j=1}^{3}\frac{q_i q_j}{r_{ij}}. \quad (1)$$

Where ε_{ij}, σ_{ij}, and q_i are the characteristic energy, size parameters, and partial charge respectively, r_{ij} is the distance between the center of mass of the pair of atoms.

The Lorentz-Berthelot mixing rules: $\sigma_{ij} = (\sigma_i + \sigma_j)/2$ and $\varepsilon_{ij} = \sqrt{\varepsilon_i \varepsilon_j}$ are used for unlike intermolecular interaction. A cut off radius of 12 Å is used for Lennard-Jones interactions. Long range electrostatic interactions are incorporated using the particle-particle-particle mesh (pppm) methods. Bond stretching and angle bending are described by harmonic potential.

$$U_{stretching} = \frac{1}{2}k_l(l - l_0)^2, \quad (2)$$

and

$$U_{bending} = \frac{1}{2}k_\theta(\theta - \theta_0)^2, \quad (3)$$

where k and k_θ are force constants, l, θ, l_o, and θ_o are bond length, bond angle, and their corresponding equilibrium values respectively.

The DFT partial charges for DB18C6 [30] are determined by performing an ab initio quantum chemistry calculation with B3LYP/6-31+G* level of theory. Additional force field parameters for DB18C6 are reported in Tables S1 and S2. All simulations are conducted using Nosé-Hoover thermostat and barostat at the constant temperature T=298 K and constant pressure 1 atm with an integration time step of 1 fs.

Methods

The structural properties of the ion-solvent complex are described by the pair correlation function *g(r)*.

$$g(r) = \rho^{-2}\left\langle \sum_i \sum_{j\neq i} \delta\left(r - r_j\right)\right\rangle = \frac{V}{N^2}\left\langle \sum_i \sum_{j\neq i} \delta\left(r - r_{ij}\right)\right\rangle, \quad (4)$$

where ρ, N, V, and δ represent number density, total number of molecules in the system, total volume, and kronecker delta respectively.

The average number of particles of type i around the particle of type j in the first solvation shell, is given by coordination number (CN), which is obtained by integrating $r^2 g(r)$ up to first minimum of pair correlation function [31]

$$N_1 = 4\pi \int_{r_0}^{r_1} r^2 g(r)\rho dr, \quad (5)$$

Where r_0 is the rightmost position starting from $r = 0$ where *g(r)* is approximately zero and r_1 is the first minimum.

Self-diffusivity (D) in this work is evaluated based on Einstein relation, where diffusion coefficient is related to the slope of mean square displacement (MSD) of particles over time [32].

$$2dD = \lim_{t\to\infty} \frac{d}{dx}\left\langle \left|R(t) - R(0)\right|^2\right\rangle, \quad (6)$$

where *R(t)* and *d* denotes the coordinates of ion at time t and dimension of the system respectively.

The velocity auto correlation function (VACF) of Li^+ has been compared in different solvents using quantity $\langle v(t')\cdot v(t'')\rangle$, which measures the correlation between the velocity of the particle at time t' and t''. The angular brackets indicate an average over time.

Hydrogen bond (HB) interactions between DB18C6 and solvent species have been checked with three geometrical conditions as per reference [31–33].

Potential of mean force (PMF) is calculated in order to demonstrate the stability of DB18C6/Li^+ complex in the solvents using the following formalism [34, 35].

$$V(r) = -k_B T ln(g(r)), \quad (7)$$

where pair correlation function g(r), corresponds to interaction between Li^+ and center of mass (COM) of solvent molecules.

Orientation of solvent species at the interface of immiscible liquids is evaluated using the order parameter [36]:

$$S = \left\langle 0.5\left(3\cos^2\theta - 1\right)\right\rangle, \quad (8)$$

where $_\theta$ is the angle between Z-axis and either dipole moment of water molecules, C-H vector of chloroform or C(N)-N vector of nitrobenzene. S vector is averaged over time and over all solvent molecules present in dynamically defined slabs of 1 Å parallel to the interface. Orientation profile [37] for DB18C6 with respect to interface is given by probability density P($_\theta$, r). In our study, $_{\theta 1}$ has been described as an angle between X-axis and vector1 (v1) and $_{\theta 2}$ as an angle between vector1 (v1) and vector2 (v2), where v1 and v2 join the center of mass (COM) of cavity to the COM of 1st and 2nd benzene rings respectively.

Simulation details

Simulations are performed using LAMMPS [38] molecular dynamics package for the systems containing Li^+/solvent and Li^+/DB18C6/solvent. Solvents used in this study are water, methanol, chloroform, and nitrobenzene. These systems are simulated in a cubic box containing 800 molecules of solvent (water, methanol, chloroform, and nitrobenzene respectively) and 20 solute molecules (DB18C6, Li^+) using periodic boundary conditions in x, y, and z dimensions.

The MD simulation of Li^+/DB18C6 at aqueous/organic interface is started with two adjacent cubic boxes, containing 800+250 (water + organic) molecules for $(Li^+/DB18C6)_6$ solute under periodic boundary conditions in all dimensions (Table S3). Cl^- and NO_3^- have been used as counter-ions. After 10,000 steps of a conjugate gradient minimization, the systems were allowed to equilibrate for 1 ns (solute/solvent systems) and 5 ns (interface systems) before the production runs of 10 ns (solute/solvent systems) and 20 ns (interface systems) were performed. All simulations have been

performed using Nosé-Hoover thermostat and barostat at 298 K and 1 atm, with a time step of 1 fs.

Results and discussion

DB18C6/Li^+ complex in water: cation shielding and dynamic behavior

Hydration structure of DB18C6/Li^+ complex in water

The structure of the solvent molecules around an ion is described by the RDF and CN. The RDFs of Li^+ in bulk and DB18C6/Li^+ complex are shown in Fig. 1. It is observed that the value of $g_{Li\text{-}Ow}$ in complex is zero in the first solvation shell, which corresponds to ~2.0 Å in bulk solution. In other words, in the presence of DB18C6/Li^+ complex, the first solvation shell is observed at ~4.2 Å, equivalent to second solvation shell (~4.4 Å) in bulk solution (see Fig. 1a). Also, the peak height of the RDF in the DB18C6/Li^+ complex is lower than that in bulk solution. This is due to the dehydration of Li^+ during complex formation within the cavity of DB18C6, i.e., DB18C6 replaces some water molecules from the solvation shell of the Li^+ [39]. However, the Li^+ in DB18C6/Li^+ complex, is not completely dehydrated but surrounded by 1–3 water molecules in their first solvation shell as per coordination number profile [31]. In the presence of DB18C6, the RDF peak for Li^+-Hw is noticed prior to Li^+-Ow, which is in contradiction to the pattern seen in the aqueous LiCl solution (where the Li^+-Ow peak is noticed prior to Li^+-Hw, because O atoms of water molecules point toward the Li^+ due to the electrostatic interactions) as shown in Fig. 1b. This indicates weaker coordination of Li^+ with water molecules where HB interactions between Oc-Hw [14] dominates over shielded electrostatic interaction between Li^+-Ow [15]. Figure 1c represents the averaged distribution of Li^+-Oc distances. The Li^+-Oc distance is found to be ~2.175 Å and one Li^+ is surrrounded by six oxygen atoms of DB18C6. The distribution observed in this work is similar to K^+/18C6(O) system, studied by Mazor et al. [40] for K^+/18C6 in methanol using the MM force field, and by Leuwerink et al. [41] in the MM/MD study of 18C6 with Na^+, K^+, and Rb^+ ions. The sharpness of these distributions indicates a good fit of Li^+ ion in the cavity of DB18C6 [42].

Dynamic behavior of DB18C6/Li^+ complex in water

The effect of complexation on the dynamics of Li^+ by DB18C6 is given by the calculated VACF and MSD profiles from MD simulation. Li^+ is shown to lose its free translational motion when it is bound by DB18C6 as clearly evident from Fig. 2a. Appearance of damped oscillations in the VACF profile (Fig. 2b) of complexed Li^+ indicates the high frequency motion of the Li^+ in a cage of DB18C6. Further, MSD curves are used for the calculation of diffusion coefficient and it has been found that the diffusion coefficient of Li^+

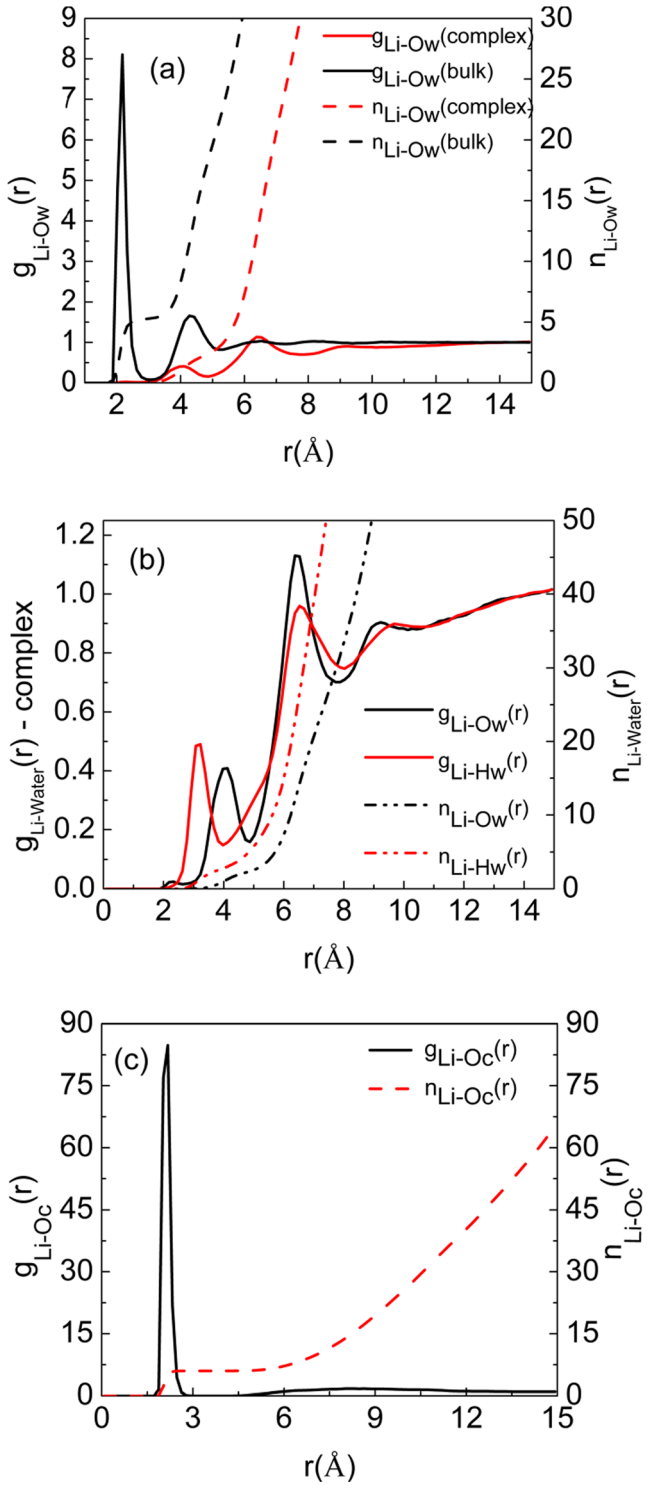

Fig. 1 **a** Comparison of RDF and CN of Li^+-Ow in DB18C6/Li^+complex-water (*red*) with bulk water (*black*). **b** RDF and CN of Li^+-Ow (*black*) and Li^+-Hw (*red*) in DB18C6/Li^+complex-water. **c** RDF and CN of Li^+-Oc in DB18C6/Li^+-water, where Oc is oxygen of DB18C6

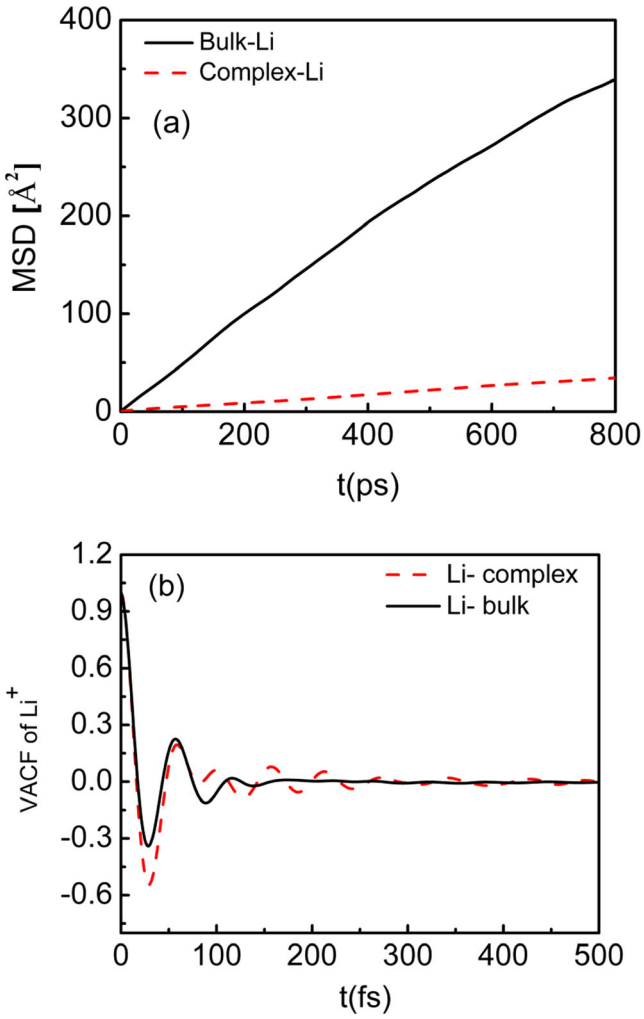

Fig. 2 Comparison of (**a**) Mean square displacement (MSD) (**b**) Velocity autocorrelation function (VACF) of Li^+ in bulk water (*black*) and DB18C6/Li^+ complex-water (*red*)

is reduced substantially in the presence of DB18C6 compared to bulk water as shown in Table 1.

Effect of solvents: cation shielding from solvent and relative stabilities

The transfer of metal ions from aqueous solution to the organic solvents without ligand assistance is not thermodynamically favorable but complexation with DB18C6 facilitates their extraction in organic solvents as observed in the liquid-liquid extraction process. Since this complexation and decomplexation reaction depends on the environment [43] and conformation of crown ether, appropriate choice of solvent becomes an important issue for the extraction of metal ions. In this study, we have used water, methanol, chloroform, and nitrobenzene as solvents. Water and methanol are used to demonstrate the effect of aqueous and alcoholic medium respectively; chloroform represents simple organic solvent with easy availability and nitrobenzene (NBZ) as a representative of aromatic solvents.

Table 1 Diffusion coefficient for Li^+

System	D/10^{-5} (cm^2/sec)
Bulk water	0.78±0.00012
DB18C6/Li^+-water	0.015±0.00029
DB18C6/Li^+-methanol	0.282±0.00056
DB18C6/Li^+-chloroform	0.309±0.00457
DB18C6/Li^+-nitrobenzene	0.301±0.00345

Figure 3a displays the RDF of Li^+ in different solvents, which clearly shows the shielding of Li^+ from solvents due to the presence of DB18C6, where the first peak height is smaller than the second peak. The local structure of solvent molecules surrounding Li^+ is changed due to the presence of DB18C6 and the solvent molecules reorganize their positions around the complex. According to RDF, water and methanol molecules are found to be closer to the DB18C6/Li^+ complex than chloroform and nitrobenzene, which is due to HB interaction of DB18C6 with water and methanol. However, the HB interaction between DB18C6 and water/methanol is very weak as the average number of HB per DB18C6 molecule is found to be 1.97 and 0.82 for water and methanol respectively. In spite of weaker HB interaction, the initial decay of HB correlation function is found to be slower for methanol than water (Fig. S4) because at short times, the linear HB chains of DB18C6-methanol are more stable than the multi-dimensional HB networks of DB18C6-water [44]. The appearance of the first NBZ molecule from DB18C6/Li^+ complex is found at a distance of 8.54 Å, quite far from the complexed Li^+, which is due to steric repulsion between NBZ and DB18C6. The RDF of Li^+-NBZ has only one peak with a value higher than one, corresponding to CN of 16.14. For water, methanol, and chloroform the average CN is found to be 2, 1.2, and 1.7, respectively. The results for CN of water and methanol centered at Li^+ are found to be in good agreement with the reported literature [45, 46]. However, to the best of our knowledge, coordination of chloroform and nitrobenzene around DB18C6/Li^+ complex has not been reported earlier.

Positions of Li^+ in DB18C6/Li^+ complex remain unaffected by their surrounding solvent molecules as shown by RDF $g_{Li/DB18C6\text{-}O}$ (Fig. 3b). Also, the average coordination of DB18C6-O around Li^+ is found to be 6 for each solvent, corresponding to 1:1 complexation of DB18C6/Li^+ in each solvent.

Further, the stability of the complex in each solvent is evaluated with the help of PMF as shown in Fig. 4. Each PMF profile exhibits two local minima; first minima correspond to the direct contact of Li^+ with solvent (CIS) while the second minima correspond to ligand (DB18C6) separated Li^+-solvent (LSIS) complex. The calculated values for local

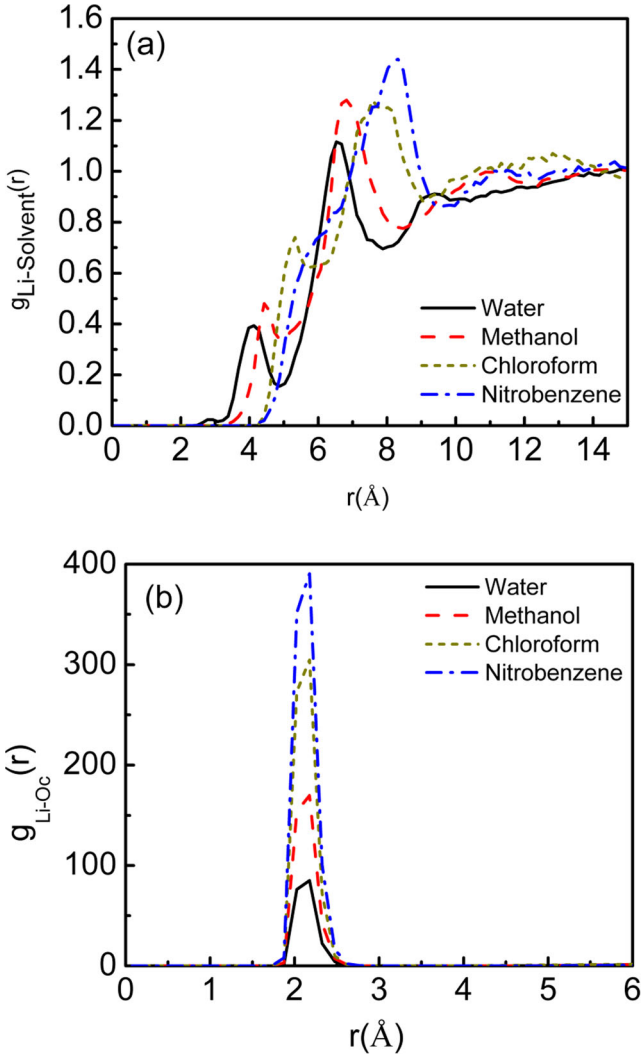

Fig. 3 RDF of (**a**) Li^+-COM of solvents (**b**) Li-Oc; where Oc is oxygen of DB18C6. (COM = center of mass of solvent molecules)

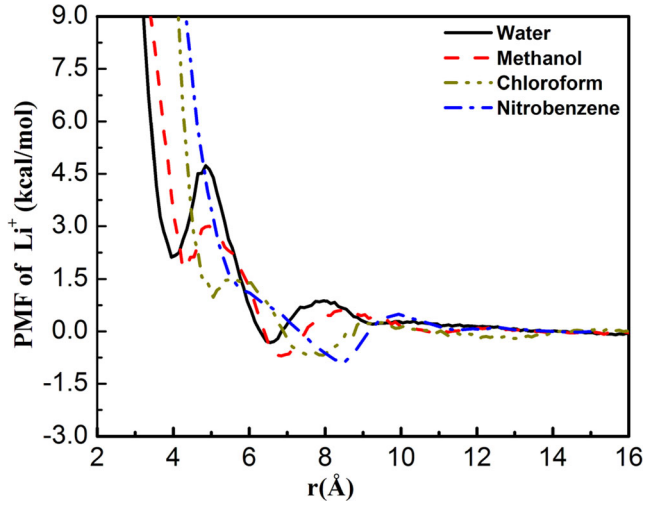

Fig. 4 Potential of mean force (PMF) of Li^+ in different solvents

minima and free energy barrier are reported in Table 2. Energy barrier for CIS is shown to be decreased in the following order: water > methanol > chloroform. However, no CIS has been observed in the case of NBZ, indicating that no Li^+-NBZ CIS complex exists at the ambient condition. The activation energy barrier for water is found to be higher than that of other solvents indicating a large amount of energy is required to remove DB18C6 from Li^+/DB18C6/water complex, which is due to strong electrostatic interaction of Li^+ with DB18C6 and decreasing HB interaction of DB18C6 with water, methanol, and chloroform respectively. In addition, for each solvent, Li^+-solvent CIS complex are thermodynamically less stable than Li^+-solvent LSIS complex, where the difference in free energy between the two local minima is found to be: 2.44, 2.50, and 1.68 kcal mol^{-1} for water, methanol, and chloroform respectively. A large depth minimum for LSIS complex indicates that the solvent shielded complex of Li^+/DB18C6 are the predominant complex in solution at equilibrium [35, 47]. Because of this weak and indirect interaction between Li^+ and solvent molecules, the orientation of DB18C6/Li^+ complex remains unaffected by the nature of solvent molecules in the surrounding.

Next, we demonstrate the effect of solvent molecules on the dynamics of complex by analyzing the VACF and MSD profiles as shown in Fig. 5a and b. In general, the effect of solvents on the diffusion of solute is given in terms of the relation [48] $D = const \times \left(\frac{TM^{1/2}}{\eta V^{0.6}}\right) t$.

where T, M, , and V represent temperature, molecular weight, viscosity and molar volume of solvent molecules respectively. However, solvent molecules having HB donating behavior do not follow this relation. Waldeck and coworkers [49] rationalized the trend of diffusion coefficient in terms of changes in 'dielectric friction' associated with different solute and solvent species. They have concluded that all these factors together determine the diffusion coefficient. In this study, diffusion coefficient is calculated using MSD profiles and the calculated values are reported in Table 1. Diffusion coefficient of complex is found to be smallest in water, which may be due to the 3D network of HB in water. However, the pattern for diffusion of DB18C6/Li^+ complex, as given by VACF profile (Fig. 5b), is found to be almost similar in each solvent.

Dynamics of Li^+ and DB18C6 at interface

Distribution with respect to interface

In this section, we report the simulated results of the Li^+ complex of DB18C6 at the interface of two immiscible solvents in order to explore the time evolution, micro-surroundings, and distribution with respect to the interface. The system is started with the conditions closer to the experimental one; in

Table 2 Calculated potential energy minima, maxima, and free energy barriers in kcal mol^{-1}

Solvent	CIS min	LSIS min	CIS/LSIS max	CIS → LSIS ΔE	LSIS → CIS ΔE	ΔE between local min (CIS and LSIS)
Water	2.12	−0.31	4.73	2.60	5.05	2.44
Methanol	1.79	−0.70	2.99	1.20	3.70	2.49
Chloroform	0.97	−0.71	1.51	0.54	2.22	1.68
Nitrobenzene		−0.85				

which Li^+ is taken in the aqueous phase while DB18C6 in the organic phase. We have performed the simulations for two sets of organic solvents — chloroform and nitrobenzene. In both cases, DB18C6 and Li^+ are shown to be moved toward the interface [50], where DB18C6 formed complex with Li^+. Figure 6a-d display the final positions of DB18C6, Li^+, and the corresponding density profile, showing that DB18C6 and DB18C6/Li^+ complex reside at the interface.

In order to explore the dynamics of DB18C6, Li^+, and DB18C6/Li^+ complex with respect to interface, position of the Li^+ and DB18C6 are monitored by calculating the distance

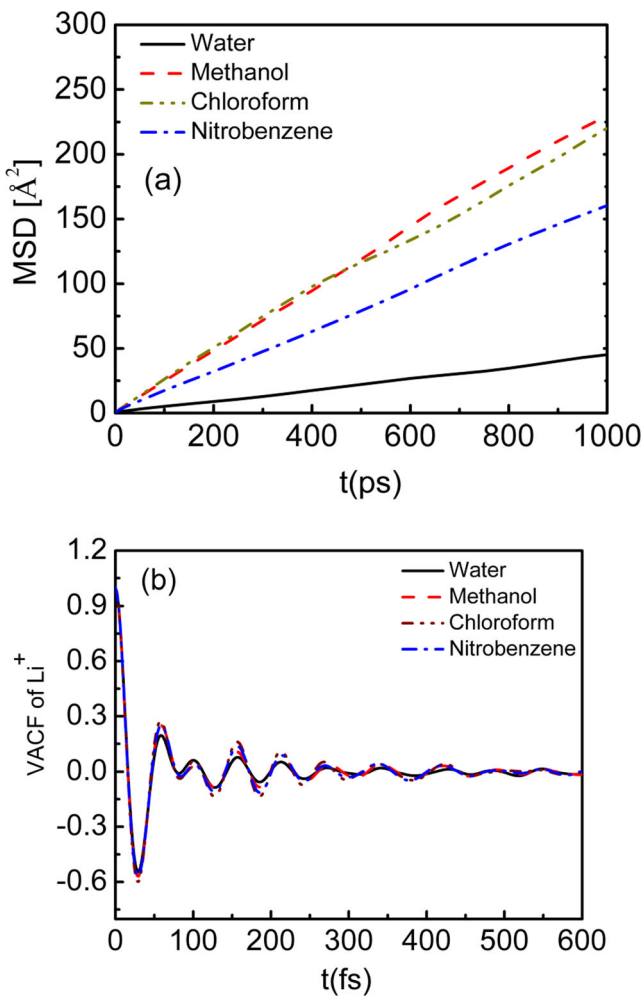

Fig. 5 **a** Mean square displacement (MSD) **b** Velocity autocorrelation function (VACF) of Li^+ in different solvents

d_i between their center of mass and the interface as shown in Fig. 7 (corresponding to $(DB18C6)_{CHCl3}/(Li^+)_{H2O}$). The time evolution of d_i shows that within 0.4 ns, all the DB18C6 and Li^+ came at the interface of water/chloroform and then they formed complex, which quantifies the fact that the energy barrier for complex formation is minimum at the interface as compared to bulk solutions. After the dynamics of 2–3 ns all DB18C6 are found to be in the DB18C6/Li^+ complex form. On the other hand, in the case of water/nitrobenzene system, some (~16 %) DB18C6 and Li^+ are found to be free (no complexation) even after the dynamics of 20 ns. The reason for this dissimilarity might be explained in terms of polarity of the organic solvent; chloroform provides higher complex formation rate as compared to nitrobenzene due to its high polarity. It has been observed that complexed Li^+ remains close to the interface in DB18C6/Li^+ complex form while the uncomplexed Li^+ diffuses back to the bulk water. However, DB18C6 molecules prefer to be at the interface no matter whether they are uncomplexed or complexed with Li^+ due to their amphiphilic nature. In other words, aromatic rings of DB18C6 having hydrophobic character, remain solvated by organic solvent while oxygen impregnated DB18C6-cavity is expelled toward aqueous phase due to their hydrophilic nature. Encapsulation of cation in the cavity of the crown ether enhances the hydrophilic characteristics of DB18C6 and hence force them to stay at the interface.

Overlapping of trajectory for one Li^+ over one DB18C6 (see Fig. 7), corresponds to the 1:1 complex formation by DB18C6 and Li^+ during solvent extraction process.

In order to study the effect of counter-ions, we have carried out two more simulations including Cl^- and NO_3^-. Due to similar electrostatic nature and almost equal molar volume, both the counter-ions Cl^- and NO_3^- show same behavior for water/organic interface. Hydrophilic anions Cl^- and NO_3^- initially follow Li^+ as an intimate ion pair. However, once the Li^+ forms complex with DB18C6, they dissociate and diffuse back to the water phase [51] (see Fig. 8). However, a competition has been observed between Cl^- and DB18C6 for Li^+. During the dynamics of 20 ns, many of the Cl^- are found to be in DB18C6/Li^+/Cl^- complex form at the water/organic interface, facing Cl^- toward water. However, none of the Cl^- is found to remain associated with DB18C6/Li^+ complex during 20 ns simulation as observed earlier by Varnek et al. [52].

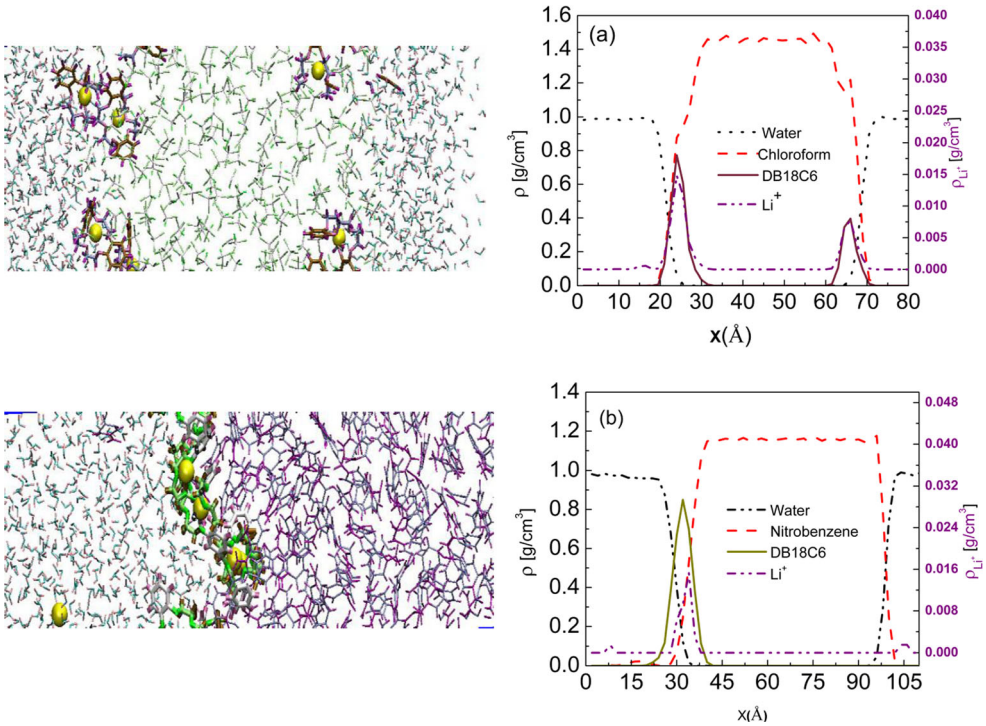

Fig. 6 Snapshot and density profile of (**a**) water/chloroform and (**b**) water/nitrobenzene system with DB18C6 and Li^+. (ρ_{Li} is density of Li^+)

Molecular structure and dynamics at interface

In this section, we have focused on the properties like order parameter (S) and orientation probability ($P(_{\theta,}r)$); that directly reflect the microscopic behavior of molecules at the interface region and hence provide valuable information about the microscopic environment at the liquid-liquid interface. $S \neq 0$ indicates anisotropic orientation of molecules. Because of asymmetry in the forces experienced by solvent molecules at the interface, they have preferential orientation and hence the orientation of the solvent molecules at the interface is anisotropic [36] while it is isotropic in their bulk domains as indicated by the Fig. 9a-b.

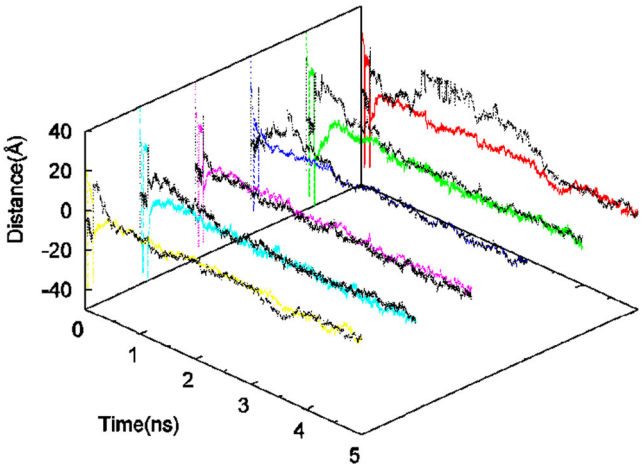

Fig. 7 Distance between different DB18C6 (*color*) and Li^+ (*Black*) from water/chloroform interface

The orientation profiles for DB18C6 in water/chloroform and water/nitrobenzene are shown in Fig. 10, where the highest probability is found to be at $_{\theta 1}$≈70–90° and $_{\theta 2}$≈110–120°. In case of water/nitrobenzene system an additional peak was observed at ~150°, corresponding to uncomplexed DB18C6 (~16 % DB18C6 were found to be uncomplexed in the case of water/nitrobenzene system). Based on these results, it is predictable that DB18C6 prefers parallel orientation ($_{\theta 1}$≈70–90° w.r.t. to x axis or $_{\theta 1}$≈0–20° w.r.t. to interface) with respect to water/organic interface, to allow the precise interaction of hydrophilic sites of the solute with aqueous phase. Encapsulation of Li^+ inside DB18C6, results in restructuring of the DB18C6-cavity as the angle $_{\theta 2}$ was reduced to ~115° from 150°, during DB18C6/Li^+ complex formation [39]. The deformed geometry of DB18C6/Li^+ is also responsible for its strong complexation capacity for Li^+, which prevents their dissociation even at asymmetrical environment. This is the reason, that once DB18C6 formed complex with Li^+, it did not dissociate further even at higher concentration of DB18C6 and Li^+ at the interface, which is in contradiction to the behavior reported for 18C6/Li^+ complex [50].

Figure 11 represents the distribution of solvent molecules around the extracted Li^+. Complexed Li^+ is found to be surrounded by 1–2 water molecules and 6–8 water molecules in their first solvation shell (~3.75 Å) and second solvation shell (~6.75 Å) respectively at water/organic interface. Average number of organic solvents in the surrounding of extracted Li^+ is negligible (the first solvation shell for organic solvents has been observed at ~7.25 Å and ~8.15 Å for water/

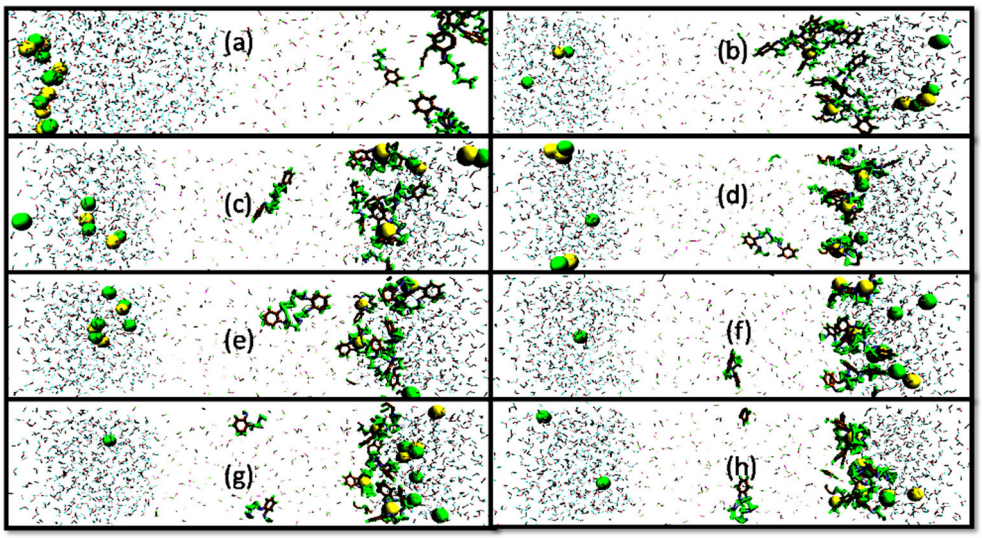

Fig. 8 Snapshots of solutes (DB18C6, Li^+, and Cl^-) and solvents (water and chloroform) species with respect to interface at time (**a**) 0.0 ns (**b**) 1.5 ns (**c**) 2.5 ns (**d**) 5 ns (**e**) 10 ns (**f**) 12 ns (**g**) 17 ns and (**h**) 20 ns

chloroform and water/nitrobenzene respectively). These results display higher interaction of DB18C6/Li^+ complex with water rather than organic solvent. Based on these results, it could be anticipated that the complex should move to the aqueous phase rather than being at the interface, opposite to our findings. However, that is not observed within 20 ns of simulation time. The reason for this disagreement is attributed to the surface tension. Since water has surface tension much higher than both of the organic solvents (72.9, 26.7, and 43.9 mN/m for water, chloroform, and nitrobenzene respectively), energy cost for creating a cavity in water is higher than the organic solvents, which is too large to be compensated by complex-water interactions. On the other hand, while staying at interface, the solute (DB18C6/Li^+ complex) still enjoys significant stabilizing interactions with the aqueous phase.

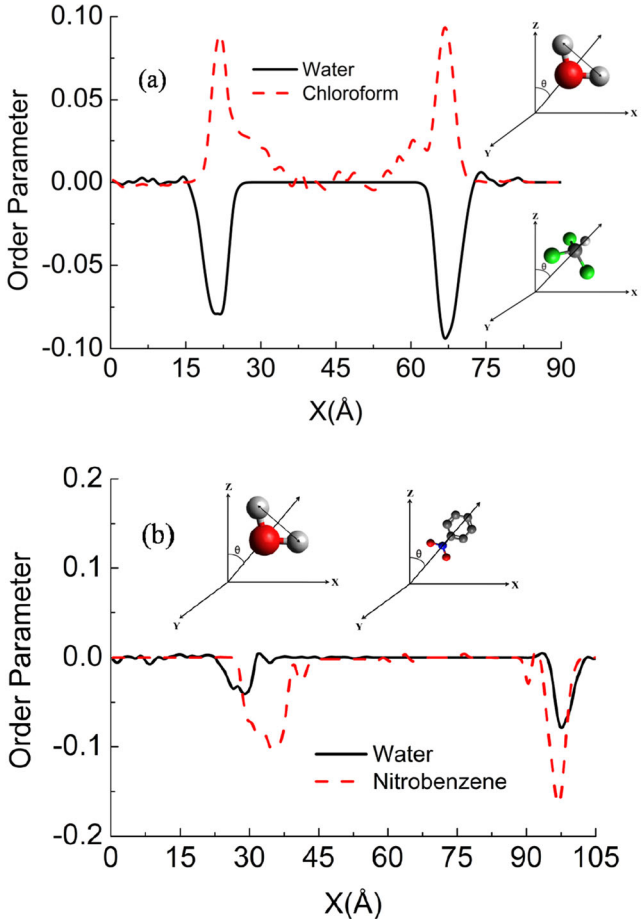

Fig. 9 Order parameter for (**a**) water/chloroform (**b**) water/nitrobenzene

Conclusion

We have reported the theoretical study using MD simulation for the extraction of Li^+ using DB18C6 in various solvents. DB18C6 acts as an extracting molecule and spontaneously forms complex with Li^+ in all the simulated systems. The effect of different organic solvents on the structure and

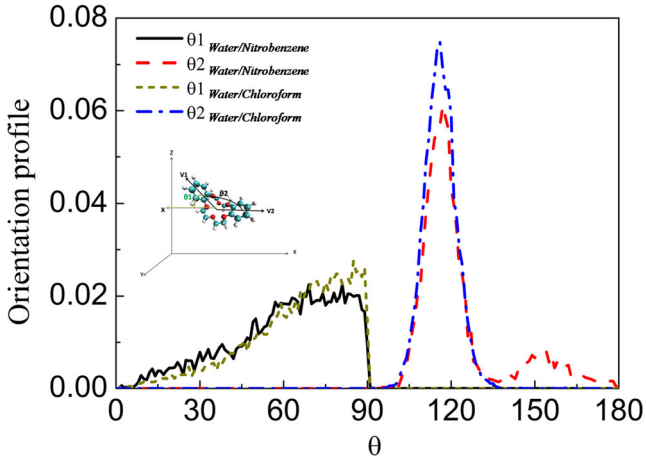

Fig. 10 Orientation probability of DB18C6 for different water/organic interface

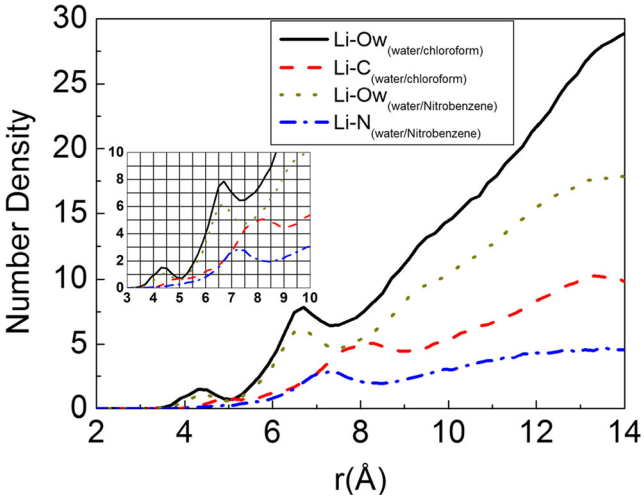

Fig. 11 Number density of solvents around encapsulated Li^+ for water/chloroform and water/nitrobenzene systems. Ow, C, and N are oxygen of water, carbon of chloroform, and nitrogen of nitrobenzene respectively

dynamics of DB18C6/Li^+ complex compared to water have been reported using methanol, chloroform, and nitrobenzene. Also, to the best of our knowledge, this is the first MD simulation study on the complexation of DB18C6 and Li^+ in different organic environments as well as in aqueous/organic interface. It can thus be considered as an important step toward realistic simulation of liquid-liquid extraction for Li^+ using DB18C6. In the presence of DB18C6, a shift in the solvation shells of lithium ion was observed due to boat like structure of DB18C6/Li^+ complex, leading to shielded solute-solvent interaction. For instance, DB18C6 encapsulated Li^+ ions showed the RDF peak of $g_{Li\text{-}Hw}$ prior to $g_{Li\text{-}Ow}$, in contrast to the behavior observed in the bulk LiCl solution. This might be due to hydrogen bond (HB) interaction between Oc (O of DB18C6) and H (hydrogen of solvents viz: water and methanol) and hence plays an important role in the extraction of solvated metal ion complex. Solvent-complex interaction was found to be in the decreasing order of water, methanol, chloroform, and nitrobenzene, respectively, as supported by PMF profiles. The results indicate that the presence of methanol in the aqueous phase would favor the ion extraction whereas chloroform will be a better co-solvent than nitrobenzene. In addition, a larger depth minima for LSIS than CIS, indicates that the solvent shielded complex of Li^+ with DB18C6 is the predominant complex in the solution.

Further, the studies were extended to water/organic interface to mimic the experimental system; in which Li^+ was taken in the aqueous phase while DB18C6 in the organic phase. Chloroform and nitrobenzene was chosen as the modeled organic solvents. The present simulation results demonstrate that the DB18C6 are surface active and therefore bear strong analogies like micelles to form amphiphilic complex. This is a favorable feature as far as the mechanism of ion capture is concerned. Also, the non-zero order parameter of solvent species at interface, enhances the ion extraction by reducing the surface tension of interface. Indeed, the lower surface tension of interfacial region not only favors the complex formation but also prevents their migration toward aqueous phase irrespective of increased hydrophilic character of DB18C6 after complex formation. In addition, the complexes were found to be preferred in the parallel orientation with respect to interface with their aromatic rings solvated by organic phase while hydrophilic cavity facing toward aqueous phase. The complex thus enjoys the significant stabilizing interaction with aqueous phase, while staying at interface.

During the dynamics, many Cl^- counter ions were found at the interface, in the form of DB18C6/Li^+/Cl^- complex where Cl^- faces the water. However, none of the complexes formed with Cl^- were found to be stable during the complete 20 ns simulation due to their sturdy hydrophilic character. Also, a competition was observed between Cl^- and DB18C6 to intimate the Li^+. Based on these results it can be predicted that counter ion with hydrophobic nature and bulky mass (for massive and larger molecules, it would be difficult to break the surface tension of water to remigrate to aqueous phase) would be required to facilitate the approach of ion to the interface and crossing the phase boundary by forming an overall neutral hydrophobic complex.

Overall, present simulation results provide microscopic pictures of solute/solvent interactions for bulk solvent and solvent/solvent interface and thus provide a deeper understanding of assisted ion extraction which remains unclear from experiments alone. We firmly believe that the present study would be very supportive for the experimentalist to avoid the extra efforts in solvent selection and use of appropriate amount of extractant by knowing the stoichiometry of the metal-ligand complex (as predicted here 1:1 complex formation behavior of DB18C6 and Li^+). Effect of solvent on molecular recognition might also be supportive for various related fields such as catalysis, electrochemistry, and ion exchange through membranes.

Acknowledgments This research was done at IIT/Kanpur under DGFS fellowship, supported by BRNS project.

We are grateful to IIT Kanpur HPC for computational support. We are also thankful to Anitha K. of IIT Kanpur, Dr. S.K. Ghosh, Director ChEG and Dr. K.T. Shenoy, Head ChED of BARC for their continuous encouragement and support.

References

1. Tarascon JM, Armand M (2001) Issues and challenges facing rechargeable lithium batteries. Nature 414(6861):359–367
2. Bauer M, Forsthoff A, Baethge C, Adli M, Berghofer A, Dopfmer S, Bschor T (2003) Eur Arch Psychiatry Clin Neurosci 253:132–139
3. Fumo N, Goswami DY (2002) Study of an aqueous lithium chloride desiccant system: air dehumidification and desiccant regeneration. Sol Energy 72(4):351–361. doi:10.1016/S0038-092X(02)00013-0

4. Stull JO, White MG (1985) Air revitalization compounds: a literature survey. Toxicol Environ Chem 10(2):133–155. doi:10.1080/02772248509357098
5. Lavernia EJ, Srivatsan TS, Mohamed FA (1990) Strength, deformation, fracture behaviour and ductility of aluminium-lithium alloys. J Mater Sci 25(2):1137–1158. doi:10.1007/bf00585420
6. Symons EA (1985) Lithium isotope separation: a review of possible techniques. Sep Sci Technol 20(9–10):633–651. doi:10.1080/01496398508060696
7. Brown PA, Gill SA, Allen SJ (2000) Metal removal from wastewater using peat. Water Res 34(16):3907–3916. doi:10.1016/S0043-1354(00)00152-4
8. Srivastava NK, Majumder CB (2008) Novel biofiltration methods for the treatment of heavy metals from industrial wastewater. J Hazard Mater 151(1):1–8. doi:10.1016/j.jhazmat.2007.09.101
9. Kadirvelu K, Thamaraiselvi K, Namasivayam C (2001) Removal of heavy metals from industrial wastewaters by adsorption onto activated carbon prepared from an agricultural solid waste. Bioresour Technol 76(1):63–65. doi:10.1016/S0960-8524(00)00072-9
10. Kurniawan, Tonni A (2006) Physico chemical treatment techniques for wastewater laden with heavy metals. Chem Eng J 118:83–98. doi:10.1016/j.cej.2006.01.015
11. Turker AR (2012) Separation, preconcentration and speciation of metal ions by solid phase extraction. Sep Purif Rev 41(3):169–206. doi:10.1080/15422119.2011.585682
12. Pedersen CJ (1967) Cyclic polyethers and their complexes with metal salts. J Am Chem Soc 89(26):7017–7036. doi:10.1021/ja01002a035
13. Inokuchi Y, Boyarkin OV, Kusaka R, Haino T, Ebata T, Rizzo TR (2011) UV and IR spectroscopic studies of cold alkali metal ion-crown ether complexes in the gas phase. J Am Chem Soc 133:12256–12263
14. Kriz J, Dybal J, Makrlik E, Budka J (2008) Interaction of hydronium ion with dibenzo-18-crown-6: NMR, IR, and theoretical study. J Phys Chem A 112(41):10236–10243. doi:10.1021/jp805757d
15. Guo X, Yudan Z, Mingjie W, Ximing W, Linghong L, Xiaohua L (2011) Theoretical study of hydration effects on the selectivity of 18-crown-6 between K^+ and Na^+. Chin J Chem Eng 19(2):212–216. doi:10.1016/S1004-9541(11)60156-0
16. Buschmann HJ, Mutihac RC, Schollmeyer E (2010) Interactions between crown ethers and water, methanol, acetone, and acetonitrile in halogenated solvents. J Sol Chem 39(2):291–299. doi:10.1007/s10953-010-9499-8
17. Buschmann HJ (1992) A comparison of different experimental techniques for the determination of the stabilities of polyether, crown ether and cryptand complexes in solution. Inorg Chim Acta 195(1):51–60. doi:10.1016/S0020-1693(00)83849-9
18. Karkhaneei E, Zebarjadian MH, Shamsipur M (2001) Complexation of Ba^{2+}, Pb^{2+}, Cd^{2+}, and UO_2^{2+} Ions with 18-crown-6 and dicyclohexyl-18-crown-6 in nitromethane and acetonitrile solutions by a competitive NMR technique using the ^{7}Li nucleus as a probe. J Sol Chem 30(4):323–333. doi:10.1023/a:1010323106004
19. Pedersen CJ (1988) The discovery of crown ethers. Science 241(4865):536–540. doi:10.1126/science.241.4865.536
20. Anderson JD, Paulsen ES, Dearden DV (2003) Alkali metal binding energies of dibenzo-18-crown-6: experimental and computational results. Int J Mass Spect 227:63–76
21. Boda A, Ali SM, Shenoi MRK, Rao H, Ghosh SK (2011) DFT modeling on the suitable crown ether architecture for complexation with Cs^+ and Sr^{2+} metal ions. J Mol Model 17(5):1091–1108
22. Heo J (2012) Theoretical studies on selectivity of dibenzo-18-crown-6-ether for alkaline earth divalent cations bull Korean. Chem Soc 33(8):2669–2674
23. Boda A, Ali SM, Rao H, Ghosh SK (2012) Ab initio and density functional theoretical design and screening of model crown ether based ligand (host) for extraction of lithium metal ion (guest): effect of donor and electronic induction. J Mol Model 18:3507–3522
24. Frensdorff HK (1971) Stability constants of cyclic polyether complexes with univalent cations. J Am Chem Soc 93(3):600–606. doi:10.1021/ja00732a007
25. Martin ME, Losa AM, Galvin IF, Aguilar MA (2006) An ASEP/MD study of liquid chloroform. J Mol Struct (THEOCHEM) 775:81–86. doi:10.1016/j.theochem.2006.07.019
26. Jorge M, Gulaboski R, Pereira CM, Cordeiro MN (2006) Molecular dynamics study of 2-nitrophenyl octyl ether and nitrobenzene. J Phys Chem B 110(25):12530–12538. doi:10.1021/jp061301j
27. Abascal JL, Vega C (2005) A general purpose model for the condensed phases of water: TIP4P/2005. J Chem Phys 123(23):234505–234517
28. Boda A, De S, Ali SM, Tulishetti S, Khan S, Singh JK (2012) From microhydration to bulk hydration of Sr^{2+} metal ion: DFT, MP2 and molecular dynamics study. J Mol Liq 172:110–118
29. Ryckaert JP, Ciccotti G, Berendsen HJC (1977) Numerical integration of the cartesian equations of motion of a system with constraints: molecular dynamics of n-alkanes. J Comput Phys 23(3):327–341. doi:10.1016/0021-9991(77)90098-5
30. Peter DJ, Grootenhuis PAK (1989) Molecular mechanics and dynamics studies of crown ether—cation interactions: free energy calculations on the cation selectivity of dibenzo-18-crown-6 and dibenzo-30-crown-10. J Am Chem Soc 111(6):2152–2158. doi:10.1021/ja00188a032
31. Impey RW, Madden PA, McDonald IR (1983) Hydration and mobility of ions in solution. J Phys Chem 87(25):5071–5083. doi:10.1021/j150643a008
32. Metya AK, Hens A, Singh JK (2012) Molecular dynamics study of vapor liquid equilibria and transport properties of sodium and lithium based on EAM potentials. Fluid Phase Equilib 313:16–24. doi:10.1016/j.fluid.2011.08.026
33. Kumar R, Schmidt JR, Skinner JL (2007) Hydrogen bonding definitions and dynamics in liquid water. J Chem Phys 126(20):204107–204112
34. Spangberg D, Rey R, Hynes JT, Hermansson K (2003) Rate and mechanisms for water exchange around Li^+(aqs) from MD simulations. J Phys Chem B 107(18):4470–4477. doi:10.1021/jp027230f
35. Duvail M, Guilbaud P (2011) Understanding the nitrate coordination to Eu^{3+} ions in solution by potential of mean force calculations. Phys Chem Chem Phys 13(13):5840–5847. doi:10.1039/c0cp02535f
36. Sieffert N, Wipff G (2007) Importance of interfacial adsorption in the biphasic hydroformylation of higher olefins promoted by cyclodextrins: a molecular dynamics study at the decene/water interface. Chem Eur J 13(7):1978–1990. doi:10.1002/chem.200601150
37. Benjamin I (1997) Molecular structure and dynamics at liquid-liquid interfaces. Annu Rev Phys Chem 48(1):407–451. doi:10.1146/annurev.physchem.48.1.407
38. Plimpton S (1995) Fast parallel algorithms for short-range molecular dynamics. J Comput Phys 117(1):1–19. doi:10.1006/jcph.1995.1039
39. Troxler L, Wipff G (1994) Conformation and dynamics of 18-crown-6, cryptand 222, and their cation complexes in acetonitrile studied by molecular dynamics simulations. J Am Chem Soc 116(4):1468–1480. doi:10.1021/ja00083a036
40. Mazor MH, McCammon JA, Lybrand TP (1990) Molecular recognition in nonaqueous solvent. 2. Structural and thermodynamic analysis of cationic selectivity of 18-crown-6 in methanol. J Am Chem Soc 112(11):4411–4419. doi:10.1021/ja00167a044
41. Leuwerink EHT, Harkema S, Briels WJ, Feil D (1993) Molecular dynamics of 18-crown-6 complexes with alkali–metal cations and urea: prediction of their conformations and comparison with data from the cambridge structural database. J Comput Chem 14(8):899–906
42. Thompson MA, Glendening ED, Feller D (1994) The nature of K^+/crown ether interactions: a hybrid quantum mechanical-molecular mechanical study. J Phys Chem 98(41):10465–10476. doi:10.1021/j100092a015

43. Robak W, Apostoluk W, Maciejewski P (2006) Analysis of liquid liquid distribution constants of nonionizable crown ethers and their derivatives. Anal Chim Acta 569:119–131. doi:10.1016/j.aca.2006.03.098
44. Padro JA, Saiz L, Guardia E (1997) Hydrogen bonding in liquid alcohols: a computer simulation study. J Mol Struct 416:243–248
45. Choi C, Heo J, Kim N (2012) Binding selectivity of dibenzo-18-crown-6 for alkali metal cations in aqueous solution: a density functional theory study using a continuum solvation model. Chem Cent J 6:1–8
46. Kusaka R, Inokuchi Y, Ebata T (2008) Structure of hydrated clusters of dibenzo-18-crown-6-ether in a supersonic jet-encapsulation of water molecules in the crown cavity. Phys Chem Chem Phys 10(41):6238–6244. doi:10.1039/b807113f
47. Fedorov MV, Goodman JM, Schumm S (2007) Solvent effects and hydration of a tripeptide in sodium halide aqueous solutions: an in silico study. Phys Chem Chem Phys 9(40):5423–5435. doi:10.1039/b706564g
48. Miyabe K, Isogai R (2013) Estimation of molecular diffusivity in liquid phase systems on the basis of the absolute rate theory. Anal Sci 29(4):467–472
49. Hartman RS, Alavi DS, Waldeck DH (1991) An experimental test of dielectric friction models using the rotational diffusion of aminoanthraquinones. J Phys Chem 95(20):7872–7880. doi:10.1021/j100173a059
50. Troxler L, Wipff G (1998) Interfacial behavior of ionophoric systems: molecular dynamics studies on 18-crown-6 and its complexes at the water-chloroform interface. Anal Sci 14(1):43–56
51. Wipff G, Lauterbach M (1995) Complexation of alkali cations by calix[4]crown ionophores: conformation and solvent dependent Na^+/Cs^+ binding selectivity and extraction: MD simulations in the gas phase, in water and at the chloroform-water interface. Supramol Chem 6(1–2):187–207. doi:10.1080/10610279508032535
52. Varnek A, Troxler L, Wipff G (1997) Adsorption of ionophores and of their cation complexes at the water/chloroform interface: a molecular dynamics study of a [2.2.2]cryptand and of phosphoryl-containing podands. Chem Eur J 3(4):552–560. doi:10.1002/chem.19970030410